Annals of Biomedical Engineering, Vol. 24, pp. 573–582, 1996
Printed in the USA.

0090-6964/96 $10.50 + .00

Ex Vivo Biomechanical Behavior of Abdominal Aortic Aneurysm: Assessment Using a New Mathematical Model

M. L. RAGHAVAN,*† MARSHALL W. WEBSTER,† and DAVID A. VORP*†‡

*Bioengineering Program, and Departments of †Surgery and ‡Mechanical Engineering, University of Pittsburgh, Pittsburgh, PA

Abstract—Knowledge of the biomechanical behavior of abdominal aortic aneurysm (AAA) as compared to nonaneurysmal aorta may provide information on the natural history of this disease. We have performed uniaxial tensile testing of excised human aneurysmal and nonaneurysmal abdominal aortic specimens. A new mathematical model that conforms to the fibrous structure of the vascular tissue was used to quantify the measured elastic response. We determined for each specimen the yield (σ_y) and ultimate (σ_u) strengths, the separate contribution to total tissue stiffness by elastin (E_E) and collagen (E_C) fibers, and a collagen recruitment parameter (A), which is a measure of the tortuosity of the collagen fibers. There was no significant difference in any of these mechanical properties between longitudinal and circumferential AAA specimens, nor in E_E and E_C between longitudinally oriented aneurysmal and normal specimens. A, σ_y, and σ_u were all significantly higher for the normal than for the aneurysmal group: $A = 0.223 \pm 0.046$ *versus* $A = 0.091 \pm 0.009$ (mean ± SEM; $p < 0.0005$), $\sigma_y = 121.0 \pm 32.8$ N/cm^2 *versus* $\sigma_y = 65.2 \pm 9.5$ N/cm^2 ($p < 0.05$), and $\sigma_u = 201.4 \pm 39.4$ N/cm^2 *versus* $\sigma_u = 86.4 \pm 10.2$ N/cm^2 ($p < 0.0005$), respectively. Our findings suggest that the AAA tissue is isotropic with respect to these mechanical properties. The observed difference in A between aneurysmal and normal aorta may be due to the complete recruitment and loading of collagen fibers at lower extensions in the former. Our data indicate that AAA rupture may be related to a reduction in tensile strength and that the biomechanical properties of AAA should be considered in assessing the severity of an individual aneurysm.

Keywords—Aortic aneurysm, Biomechanical properties, Tensile strength, Mathematical model, Fibrous structure

INTRODUCTION

It is estimated that 3–5% of the population beyond 50 years of age develop an abdominal aortic aneurysm (AAA). If left untreated, an AAA will ultimately rupture, usually with fatal consequences. At present, AAA repair requires major abdominal surgery. A reliable predictor of impending AAA rupture would be useful in determining the severity of aneurysms on an individual basis and would aid in the decision on elective surgical intervention. Although a number of risk factors have been suggested for AAA rupture based on clinical, pathological, and biochemical observations (7,8,15,19,25,31), the maximum diameter of the aneurysm is widely used as the principal criterion for elective repair (5). The major argument against using AAA diameter as the sole criterion for the probability of rupture is that some large aneurysms do not rupture, whereas some small aneurysms do (8). Clearly, the aneurysm size alone is not the best criterion for decisions regarding elective resection. From a biomechanical standpoint, AAA rupture represents the catastrophic failure of the diseased aortic wall. Knowledge of the biomechanical behavior of the aneurysmal human abdominal aorta, therefore, may further the understanding of AAA pathogenesis and rupture.

In this study we subjected freshly excised human aneurysmal and nonaneurysmal infrarenal aorta to uniaxial tensile testing. A new mathematical model is used to characterize the elastic response of the AAA and control aorta. Unlike previous models for the biomechanical behavior of arteries, ours conforms to the fibrous structure of the tissue and allows for a microstructure-based physical interpretation of the model parameters. We also report for the first time failure strengths for human AAA *versus* nonaneurysmal control aorta.

MATHEMATICAL MODEL

Soft biological tissue, including aorta, contains two primary load-bearing fibers: elastin and collagen. Elastin is characterized as compliant, whereas collagen is much stiffer (9,10,22,23). When soft tissue is load-free, the elastin fibers are taut and the collagen fibers are tortuous, or wrinkled (4,9,20,22,23). Therefore, at zero and small strains, the entire load placed upon a uniaxially loaded specimen is assumed to be borne entirely by elastin fibers. The initial response of the tissue (*i.e.*, at low strains) is characterized by a linear stress-strain curve with a slope that reflects the total stiffness of the elastin fibers alone (see Fig. 1, phase 1). As the tissue is stretched, some of

Acknowledgment—The authors would like to thank Drs. David Steed, Michel Makaroun, Satish Muluk, and Ron Shapiro for supplying the human aortic tissue for experimental testing. We are also grateful Donald Severyn and Elise Dick for their technical assistance.

Address correspondence to David A. Vorp, Ph.D., Section of Vascular Surgery, Department of Surgery, University of Pittsburgh, A-1011 P.U.H., Pittsburgh, PA 15213.

(Received 13Sep95, Revised 30Jan96, Accepted 2Feb96)

the less wrinkled collagen fibers gradually become taut and start contributing to the load bearing, a phenomenon previously (1,22,23) referred to as "collagen recruitment" (see Fig. 1, phase 2). Samila and Carter (23) studied the morphology and elastic properties of human carotid arteries at various degrees of stretch and showed that as more and more collagen fibers are recruited to load bearing, the stiffness of the tissue increases. Therefore, there is a corresponding gradual increase in the slope of the stress-strain curve at medium strains (1,6,9,20,22,23). At some point prior to failure of the tissue, we assume that all of the collagen fibers are recruited into load bearing and the stiffness of the tissue reaches its maximum (see Fig. 1, phase 3). There is no further increase in slope, and the stress-strain curve is again linear until inelastic damage (yield) occurs. If we also assume that the other tissue components (*e.g.*, smooth muscle, *etc.*) do not offer significant passive load bearing (22), the slope of this final portion of the stress-strain curve corresponds to the combined total stiffness of the elastin and collagen fibers.

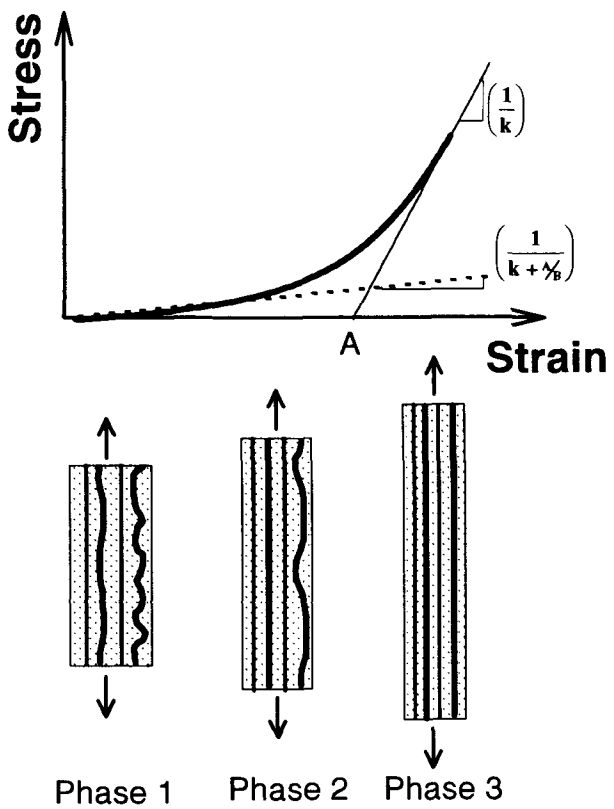

FIGURE 1. The three presumed phases of a typical elastic response (bold curve) and the corresponding hypothetical fibrous arrangement within the specimen. The thin lines in the fiber matrix represent compliant elastin fibers, and the thick lines represent stiff, variably tortuous collagen fibers. The dashed straight line on the curve is tangential to the initial linear region (phase 1) with slope equal to $1/(K + A/B)$, and the solid straight line is tangential to the final linear portion of the elastic response (phase 3) and has a slope equal to $1/K$.

In mathematical terms, for phase 1:

$$\left.\frac{d\sigma}{d\varepsilon}\right|_{\sigma\to 0_y} = \text{constant} = E_E, \tag{1}$$

where σ is the stress and ε is the strain resulting from the applied uniaxial tension, and E_E is the contribution to total tissue stiffness by elastin fibers alone. During phase 2, $d\sigma/d\varepsilon$ is not constant, but rather increases with increasing strain. For phase 3:

$$\left.\frac{d\sigma}{d\varepsilon}\right|_{\sigma\to\sigma_y} = \text{constant} = (E_E + E_C), \tag{2}$$

where σ_y represents the yield strength of the tissue and E_C is the contribution to total tissue stiffness by collagen fibers alone.

While there is no physical analogy between the two, the profile of the strain-stress curve for soft tissue is similar to that for the rate of reaction-solute concentration curve in facilitated diffusion. A form of Michaelis-Menten equation previously used to model such transport (14) was modified accordingly to arrive at the following mathematical relationship between strain and stress:

$$\varepsilon = \left(K + \frac{A}{B + \sigma}\right)\sigma. \tag{3}$$

K, A, and B are model parameters, possibly indicative of the mechanical properties of the tissue. For phase 1, as $\sigma \to 0$, $(B + \sigma) \approx B$, and from Eq. 3:

$$\varepsilon|_{\text{phase 1}} = \left(K + \frac{A}{B}\right)\sigma. \tag{4}$$

Inverting to the more typical stress as a function of strain,

$$\sigma|_{\text{phase 1}} = \frac{1}{\left(K + \frac{A}{B}\right)}\varepsilon. \tag{5}$$

Hence, Eq. 3 reduces to a linear relationship between σ and ε in phase 1 (Fig. 1). We note from Eq. 1 and Eq. 5 that

$$E_E = \left.\frac{d\sigma}{d\varepsilon}\right|_{\sigma\to 0} = \frac{1}{\left(K + \frac{A}{B}\right)}. \tag{6}$$

Let us assume *a priori* that $B \ll \sigma_y$ during phase 3, so that $(B + \sigma) \approx \sigma$ and

$$\varepsilon|_{\text{phase 3}} = K\sigma + A \tag{7}$$

or

$$\sigma|_{\text{phase 3}} = \left(\frac{1}{K}\right)\varepsilon - \frac{A}{K}. \quad (8)$$

Again the model provides a linear relationship between σ and ε in this region (Fig. 1). From Eq. 2 and Eq. 8 we note that

$$E_E + E_C = \left.\frac{d\sigma}{d\varepsilon}\right|_{\sigma\to\sigma_y} = \frac{1}{K}. \quad (9)$$

The contribution to tissue stiffness by the fully recruited collagen fibers can be found by subtracting Eq. 6 from Eq. 9:

$$E_C = \frac{1}{K} - \frac{1}{K + \frac{A}{B}} = \frac{A}{K(A + KB)}. \quad (10)$$

Physical Interpretation of the Parameters

From Eq. 9 it is seen that K is the inverse of the combined contribution to total tissue stiffness by the elastin and collagen fibers. Equation 7 indicates that A is the strain intercept of the final (phase 3) portion of the stress-strain curve (see Fig. 1). To illustrate the physical importance of the model parameter A, consider three different specimens, all with identical values of K and B, but different values of A. Model-generated stress-strain curves for three such hypothetical specimens are shown in Fig. 2. We see that as A decreases, the incremental increase in tissue stiffness with strain (*i.e.*, $d^2\sigma/d\epsilon^2$) in phase 2 increases. Based on the discussion presented above, an increased second derivative of stress with strain corresponds to a "quicker" recruitment of collagen fibers. Hence A is inversely proportional to the rate of recruitment of the collagen fibers for a given strain rate, or directly proportional to the average degree of tortuosity of the collagen fibers in the tissue. We shall refer to A as the "recruitment parameter." Interestingly, B is the value of stress at the intersection of the lines defined by the linear responses in phase 1 and phase 3 (dashed and solid lines, respectively, in Fig. 1). This is seen by equating the right-hand sides of Eq. 4 and Eq. 7. The combined effect of K, A, and B on the stiffness of elastin and collagen fibers is seen in Eq. 6 and Eq. 10.

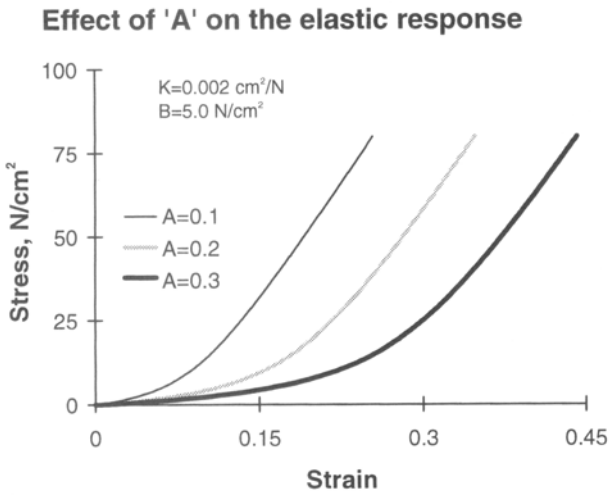

FIGURE 2. The elastic responses for three hypothetical materials, each with different values of *A*, but with the same values of *K* and *B*. Notice the greater value of $d^2\sigma/d\epsilon^2$ at lower strains for the material with lower values of *A*.

EXPERIMENTAL METHODS

Study Population

Study subjects were patients undergoing surgical repair of AAA or cadaveric organ donors. Aortic wall specimens were categorized in one of three different groups: longitudinally oriented AAA specimens (AAA_{LONG}), circumferentially oriented AAA specimens (AAA_{CIRC}), or longitudinally oriented "normal" aortic specimens from organ donors ($NORMAL_{LONG}$). Subjects were not excluded from this study based on race or sex.

Specimen Preparation

All procedures were carried out in accordance with guidelines of the NIH and the University of Pittsburgh Biomedical Internal Review Board. A segment of AAA wall (4–7 cm in length and at least 1 cm in width) was excised from patients undergoing surgical repair of their AAA. Tissue intended for AAA_{LONG} specimens were excised from the anterior aspect of the aneurysm along its long axis, whereas that intended for AAA_{CIRC} specimens was excised in an anterolateral fashion. $NORMAL_{LONG}$ tissue was obtained from remnants of infrarenal aorta following kidney transplant and was oriented along the longitudinal axis of the vessel. Circumferentially oriented specimens were not obtainable for the organ donor group because of the small transverse dimension of the remnant tissue. Immediately upon excision, the specimens were placed in saline and refrigerated at 4°C. Prior to biomechanical testing, and within 24 hours of harvest, the recovered tissue was equilibrated to room temperature by immersion in fresh warm saline. Test specimens were prepared by cutting the tissue into rectangular pieces with appropriate long-axis orientation, typically of dimensions 4 × 1 cm. The specimens were mounted in a tensile testing apparatus and continuously wetted with saline. Those pieces that were broad enough were cut into two or three adjacent pieces and individually tested.

Fifty-two longitudinally oriented (AAA_{LONG}) specimens were obtained from 45 patients aged 69 ± 2 years (mean ± SEM) with an AAA diameter of 6.3 ± 0.2 cm,

and 19 AAA_{CIRC} specimens were obtained from 16 patients aged 76 ± 2 years with an AAA diameter of 7.0 ± 0.3 cm. Seven $NORMAL_{LONG}$ specimens were obtained from the infrarenal aorta of seven cadaveric organ donors aged 47 ± 4 years.

Tensile Testing

Figure 3 shows a schematic diagram of the uniaxial testing device used in this study. This system consists of a rail table with a computer-interfaced microstepping motor (model S57-83; Parker Hannifin Corporation, Compumotor Division, Rohmert Park, CA, USA). The microstepping motor drives a five-pitch leadscrew with a resolution of 4×10^{-6} inches/step. The tees that hold the clamped specimen are supported by two brackets at opposite ends of the rail table. These brackets move in opposing directions because of rotation of the leadscrew. The functional parameters (speed, rotational direction, *etc.*) of the microstepping motor were regulated with a programmable motion controller (model AT6400 4-Axis Indexer; Parker Hannifin Corporation). A 25-lb tension load cell (model 311430-04; Sensotec, Columbus, OH, USA) is mounted at one end of the mounting brackets. An amplifier (model SA-BII: Sensotec) magnified the output signal from the load cell to 5 VDC. An A/D converter (model DT2801; Data Translations, Marlborough, MA, USA) was used to digitize the load cell output, which is subsequently stored on a dedicated microcomputer.

Aortic strip specimens from each of the three study groups were held between two clamps attached to the tees (see Figure 3). To ensure that the specimen did not slip from the clamp, cyanoacrylate glue was used between the specimen and the face of the clamp. The bracket/tee assemblies were adjusted to reach an initial length reference point for the specimen. The thickness and width of the specimen were measured at this initial length at three different positions using a dial caliper. The product of the average width and average thickness was used as the original (reference) cross-sectional area (a_o) of the specimen. To eliminate the effect of hysteresis of the tissue during the test, each specimen was preconditioned by loading to 7% strain (based on measured length changes as defined below) and unloaded repeatedly for 10 cycles at a constant strain rate of 8.5%/min. Following preconditioning, the specimen was stretched from its initial length at a strain rate of 8.5%/min until failure. Tensile force was recorded at 5 HZ using data acquisition software (Labtech Notebook, version 7.2, Data Translations). The change in specimen length for each increment of recorded load was determined from the known strain rate and the measured original length. Only specimens that failed at points remote from the clamps were analyzed and reported in this study. Data from 10 of 88 total specimens were discarded because of slipping or failure at the clamps.

Data Analysis

The load-extension data obtained during biomechanical testing were normalized to stress-strain data. The strain was defined as

$$\varepsilon = \frac{\Delta l}{l_0} \tag{11}$$

where l_0 is the original length at zero extension and Δl is the change in length at any instant. The Cauchy stress is defined as the applied force per unit area of the specimen:

$$\sigma = \frac{f}{a}, \tag{12}$$

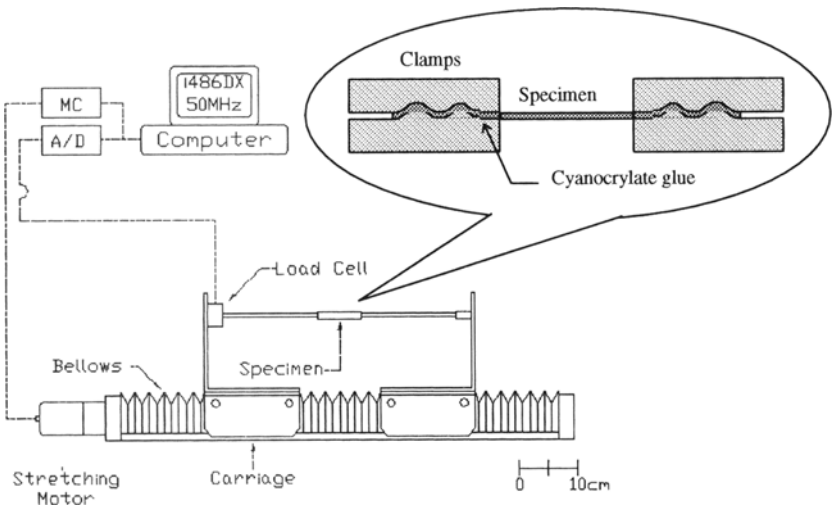

FIGURE 3. A schematic diagram of the tensile testing apparatus used for uniaxial extension of the excised aortic specimens. A motion program is sent by the microcomputer to the motion controller (MC) to operate the stretching motor. The signal from the load cell is digitized by the analog-to-digital (A/D) board and the data are stored on the computer.

where f is the force required and a is the deformed cross-sectional area of the specimen. If we assume that the aortic tissue is incompressible (3,28), the specimen volume must be preserved. That is,

$$v_0 = v, \tag{13}$$

where v_0 is the initial volume of the specimen and v is the current volume. We may approximate that

$$v_0 = a_o l_o \tag{14}$$

$$v = a\,(l_o + \Delta l). \tag{15}$$

Inserting Eq. 14 and Eq. 15 into Eq. 13 and rearranging gives

$$a = a_0 \left(\frac{l_0}{l_0 + \Delta l}\right) = \frac{a_0}{1 + \varepsilon}. \tag{16}$$

Inserting Eq. 16 into Eq. 12, we see that the stress at any given strain is given by

$$\sigma = \frac{f}{a_0}(1 + \varepsilon). \tag{17}$$

The stress-strain curve was plotted for each of the specimens tested. The yield strength, defined here as the stress at which the slope (first derivative) of the $\sigma - \varepsilon$ curve begins to decrease with increasing strain, was recorded for each specimen, as was the ultimate strength, or the maximum stress, attained prior to failure. Since it was assumed that the specimen undergoes permanent, inelastic damage beyond the yield point, only the data prior to specimen yield were considered for the parameter estimation described below.

Using a Newton-Raphson method for nonlinear regression (Statistica, version 4.5, StatSoft, Inc., Tulsa, OK), Eq. 3 was fit to the experimentally measured stress-strain data obtained for each specimen, yielding the best-fit parameters K, A, and B. Equations 6 and 10 were used to determine the properties E_E and E_C, respectively, from the model parameters for each specimen. Multiple specimens from individual patients were separately analyzed, and the parameter values were averaged to yield one value per study subject. An independent Student's t-test was performed for each of the calculated physical properties between the three groups examined in this study. Statistically significant difference was taken as $p < 0.05$.

RESULTS

Regressions of all data sets reached convergence, yielding best-fit parameters for each specimen. Standard errors of the best-fit parameters were reasonably small in all cases—2.8% of the estimated parameter value on average. Group means of each model parameter are indicated in Table 1. The recruitment parameter A for the $NORMAL_{LONG}$ group was over twice that for the AAA_{LONG} group ($p < 0.0005$). Representative experimental data and the corresponding fit of the model (Eq. 3) using best-fit parameters are shown in Fig. 4 for each of the three groups tested. The coefficient of estimation (R^2) of the model fit was greater than 0.90 for all specimens. The mean values of B/σ_y for the three groups were 0.07 for AAA_{LONG}, 0.08 for AAA_{CIRC}, and 0.07 for $NORMAL_{LONG}$. The physical properties E_E, E_C, σ_y, and σ_u determined for each specimen are shown in Table 2. No significant differences were found between AAA_{LONG} and AAA_{CIRC} specimens in these physical properties. However, the yield strength (σ_y) and ultimate strength (σ_u) for the $NORMAL_{LONG}$ group were significantly ($p < 0.05$ and $p < 0.0005$, respectively) higher than those for the AAA_{LONG} group. No significant differences were found for E_E or E_C between these two groups.

Figure 5 shows three model-generated stress-strain curves for each group based on the mean values of the model parameter estimates listed in Table 1.

DISCUSSION

We have presented a simple microstructure-based mathematical model that provides insight to the *ex vivo* biomechanical behavior of human AAA and control aorta. Importantly, the physical significance of the model parameters (namely, their relationship to the mechanical function of elastin and collagen) is relevant to the study of aneurysms. This investigation also reports and compares for the first time, to our knowledge, the failure strengths of aneurysmal *versus* nonaneurysmal tissue.

Most previous studies that have assessed the biomechanical properties of aneurysms involved direct *in vivo* evaluation from noninvasive images (13,16). These studies have shown that aortic stiffness is increased because of aneurysm formation. Although such investigations have provided information on the *in situ* behavior of the wall, the use of such data to predict the mechanical properties of the AAA wall is limited. Simplified theories to obtain

TABLE 1. Group mean model parameters

Group	K ($\times 10^{-4}$ cm^2/N)	A	B (N/cm^2)
AAA_{LONG} ($N = 45$)	39 ± 5	0.091 ± 0.009	3.90 ± 0.6
AAA_{CIRC} ($N = 16$)	25 ± 4	0.103 ± 0.02	4.47 ± 0.9
$NORMAL_{LONG}$ ($N = 7$)	30 ± 8	0.223 ± 0.046	8.93 ± 3.0

Values given as mean ± SEM.

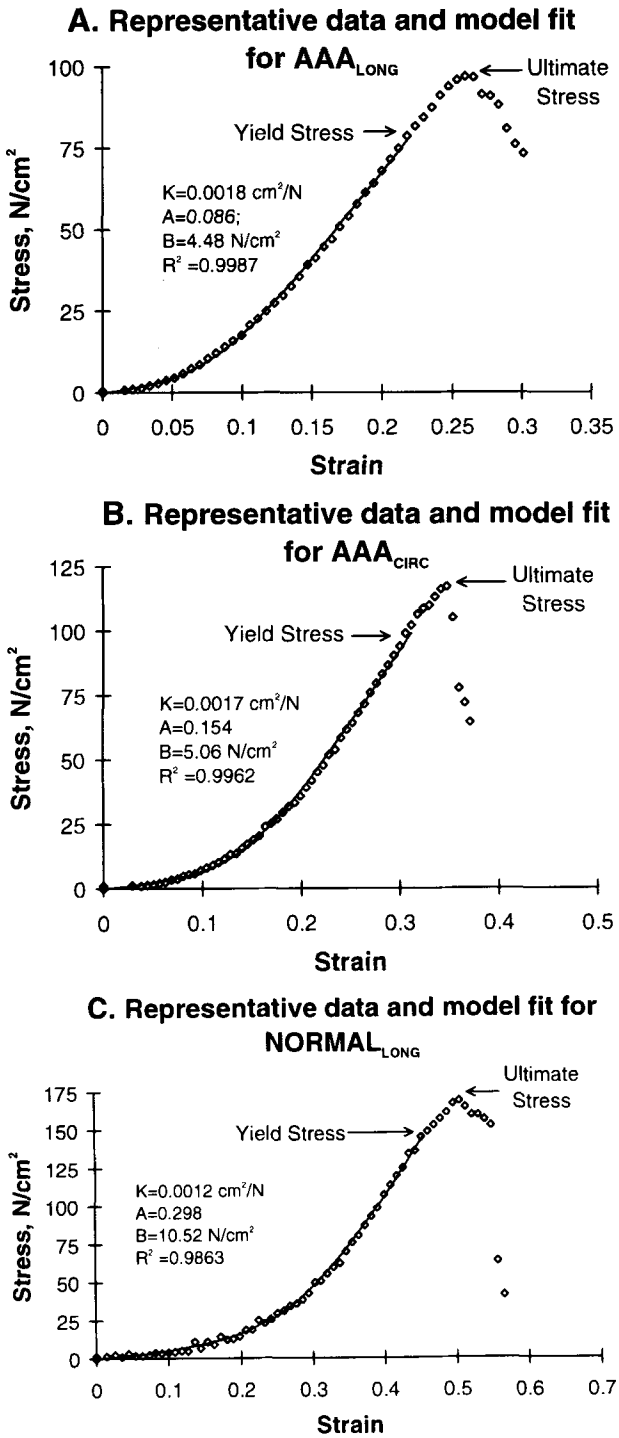

FIGURE 4. Data (symbols) and corresponding model fit from Eq. 3 (solid curve) for a single specimen representative of each of the three groups: (A) AAA$_{LONG}$; (B) AAA$_{CIRC}$; (C) NORMAL$_{LONG}$. Only the portion of the curve up to the yield point was used for parameter estimation.

stiffness were used, and the small deformation domain in which the aorta operates in the physiological range of pressure does not allow for complete material characterization. For example, the failure strengths of the aortic wall are not measurable by *in vivo* methods, and this information is important in the study of AAA rupture. *In vitro* methods involving intact AAA specimens have utilized cadaveric vessels, which are not comparable to freshly excised, viable human tissue. Both Sumner *et al.* (26) and Drangova *et al.* (11) showed that the mechanical properties of postmortem specimens of AAA were different from those of nonaneurysmal aorta and correlated these findings to histological measures of elastin and collagen content. The mechanical properties, however, were found by using pressure-circumference data. Like *in vivo* investigations, such determinations of aortic stiffness are prone to limitations, and these studies did not measure failure strengths of the studied specimens. *Ex vivo* mechanical testing of the AAA wall may yield more comprehensive information regarding the biomechanical characteristics of AAA. To date, *ex vivo* studies have been sparse. Recently, He and Roach obtained uniaxial tensile data from human AAA and postmortem nonaneurysmal abdominal aortic specimens (12). Their data suggest that the aneurysms were stiffer and less distensible than the control tissue. Like the present study (see Fig. 5), their stress-strain curves were shifted to the left for aneurysmal specimens as compared to the normal tissue. However, the specimens used in this study by He and Roach were loaded well below what we show in the present work to be typical values of yield strength. As a result, neither the full mechanical response nor the failure stress was obtained in that study. Therefore, quantitative comparisons of our results with theirs are not possible.

An important facet of biomechanical characterization of soft tissue is the mathematical model used. Previously used models for the elastic response of aortic tissue are either quite complex or limited by numerous, often questionable assumptions. The popular phenomenological hyperelasticity models (27,29,30) do not conform to the known fibrous structure of the tissue. Moreover, the many parameters often associated with these models are usually without physical meaning and are difficult to estimate from experimental data. Several microstructure-based models have been reported for soft tissue. Like the present work, some of these incorporated a multiphase elastic response. Armentano *et al.* (1) and Cox (6) each used such a model to describe the relative contributions of elastin and collagen to the stiffness of canine arteries. Pressure-diameter data were converted to a stress-strain curve that was segmented or discretized into three regions. A common limitation of these previous microstructure-based models is the lack of a single mathematical expression for the entire stress-strain relationship. It was necessary instead to discretize the elastic response and apply different mathematical characterizations for each portion of the curve. There is an underlying numerical limitation in segmenting the stress-strain curve into separate portions,

TABLE 2. Group mean physical properties

Group	E_E (N/cm^2)	E_C (N/cm^2)	σ_Y (N/cm^2)	σ_u (N/cm^2)
AAA_{LONG} (N = 45)	42.1 ± 5.5	408.2 ± 67.5	65.2 ± 9.5	86.4 ± 10.2
AAA_{CIRC} (N = 16)	55.6 ± 10.8	539.4 ± 87.5	70.7 ± 12.4	101.9 ± 16.0
$NORMAL_{LONG}$ (N = 7)	45.3 ± 15.8	468.1 ± 110.9	121.0 ± 32.8	201.4 ± 39.4

Values given as mean ± SEM.

since there is no particular point at which the curve undergoes a sudden change in shape and which may be identified as the junction between any two phases. Therefore, such visual discretization would be reasonably accurate only for curves that have three very distinct phases. In the case of tissues where the nonlinearity in the stress-strain curve is much more gradual, such as in the present case for AAA, the same curve could be discretized in many different ways, resulting in completely different parameter estimates. Such a situation is avoided by employing a single mathematical model to quantify the data.

To our knowledge, this investigation is the first to report failure strengths of aneurysmal and nonaneurysmal human aorta. The reduction by nearly 50% in the yield strength and over 50% in the ultimate strength of the aorta due to aneurysm is important in developing a new definition of a critical AAA. These tissue properties may be intrinsic to the biochemical and/or morphological changes that have occurred or are occurring in the aortic wall and may not be dependent on the AAA diameter *per se*. With advancement of the disease, the failure strengths may be progressively reduced until they are exceeded by the physiological wall stresses, resulting in rupture. The similarity in the mechanical properties of the circumferentially and longitudinally oriented specimens from AAA suggests that

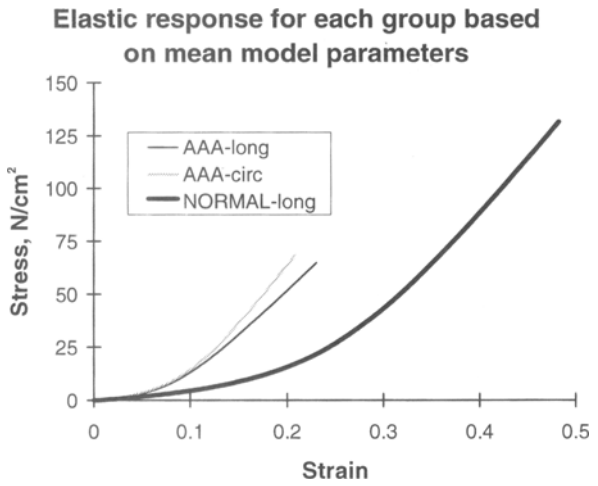

FIGURE 5. Model-generated (Eq. 3) uniaxial stress-strain curve based on the mean parameters for each group (Table 1). Peak stress in each curve represents the mean yield strength for the corresponding group.

the material is isotropic in this regard. Figure 5 illustrates the similarity in the elastic responses of specimens from these orientations. The significant difference found in the recruitment parameter of the aneurysmal *versus* control aorta suggests that the full recruitment of collagen requires greater distention or strain for the latter. This observation may reflect the changes in both geometry and fibrous structure of the aorta that accompany aneurysm development. In normal aorta, the collagen fibers are gradually recruited for load bearing because of their variably tortuous state. The greater the degree of tortuosity, the greater the strain required for all the collagen fibers to be recruited (*i.e.*, a higher value of A). Aneurysmal dilation of the aorta will cause fibers oriented in both the longitudinal and circumferential directions to decrease in tortuosity. Therefore, one may expect that less strain is required to fully recruit the collagen fibers in AAA than in normal aorta. Another possible reason for the noted differences in the recruitment parameter could be due to the structural changes known to accompany AAA formation (2,9,11,12,18,21,26). Although there is some disagreement over whether collagen content increases (11,18,21), decreases (26), or remains the same (17) with AAA, it is generally agreed that both the elastin content and elastin to collagen ratio are decreased (11,12,21,26). Both effects would tend to reduce the recoil effect of elastin and initiate the recruitment of collagen at a lower strain (9), which would result in a lower value of the model parameter A.

Our results show no significant difference in the contribution to stiffness by elastin in an aneurysmal aortic wall as compared to normal aorta. Roach and Burton (22) and Armentano *et al.* (1) suggested that the contribution to stiffness by the elastin fibers is proportional to the elastin content in that tissue. In light of our results for E_E, one would expect no difference in elastin content between our AAA and control specimens. This is not likely, based on the findings of reduced elastin mentioned above (12,21,26). Instead, this may represent a limitation in our model in simulating phase 1 of the elastic response of AAA. It was assumed in this phase that the initial load applied to the tissue is borne by the elastin alone. Since some unknown amount of collagen fibers in the aorta may become taut with aneurysmal dilation and remain so in excised specimens at zero strain, they could contribute to the initial stiffness of AAA as measured in this study. The

result could be an artificially high E_E. The mathematical model presented here has additional limitations. It is not based on principles of continuum mechanics (*e.g.*, it is not derivable from a strain energy formulation) and is suitable only to interpret uniaxial elastic responses of tissue.

The manual width and thickness measurements made with the dial calipers may have been a minor source of error in our stress calculations. However, this error would be consistent with all specimens and our comparisons should remain valid. All of the specimens in this study were harvested from the AAA close to the region of maximum dilation, which is usually the portion of the wall most susceptible to rupture (8). Data from other locations should be studied for a more comprehensive understanding of the mechanical behavior of AAA. The significant ($p < 0.0005$) difference in mean age between the $NORMAL_{LONG}$ (47 years) and AAA_{LONG} (69 years) groups is another limitation of this study. Sherebrin *et al.* (24) studied the effect of age on the stress-strain response of the human thoracic aorta. From their data we extrapolated the effect of age (from 47 years to 69 years) on the model parameters for each specimen in the $NORMAL_{LONG}$ group in the present study as follows. Based on data fit to the model,

$$\sigma = \alpha e^{\beta\epsilon}, \tag{18}$$

where α and β are the model parameters, Sherebrin *et al.* (24) found an approximately linear variation of α and β with age:

$$\alpha = -0.0166 \times (\text{age}) + 7.85 \tag{19}$$

and

$$\beta = 0.238 \times (\text{age}) + 4.00. \tag{20}$$

For a subject of age 47 years and 69 years (*i.e.*, equal to the mean age of the organ donors and AAA patients from the present study, respectively) we find $\alpha = 6.6$ and 6.1, respectively, and $\beta = 13.4$ and 18.1, respectively. Stress-strain "data" sets were generated using Eq. 18 for both ages. These "data" were then regressed against our model (Eq. 3), and the best-fit parameters were determined. We found that for the 47-year-old thoracic aorta, $A = 0.3237$, and for the 69-year-old thoracic aorta, $A = 0.2887$. This indicates that for nonaneurysmal human thoracic aorta an increase in age decreases the collagen recruitment parameter. In particular, the value of A for the 69-year-old is 12.5% less than that of the 47-year-old. If we assume that there would be a similar effect (*i.e.*, decrease in A with age) for the abdominal aorta, we may "correct" each value of A estimated for the $NORMAL_{LONG}$ specimens to provide an age-matched comparison to the AAA_{LONG} specimens. Table 3 shows the collagen recruitment parameter for each $NORMAL_{LONG}$ specimen as assessed by our methods and those corrected to 69 years based on the data of Sherebrin *et al.* An independent Student's *t*-test indicates that the corrected value of A for the $NORMAL_{LONG}$ group remains significantly higher than that for the AAA_{LONG} group: 0.195 ± 0.043 *versus* 0.091 ± 0.009 ($p < 0.005$).

TABLE 3. Age matching[a] for collagen recruitment parameter *A*

Donor	Age	A[b]	A corrected[c]
1	47	0.132	0.116
2	31	0.294	0.231
3	34	0.193	0.155
4	60	0.088	0.084
5	48	0.126	0.111
6	58	0.429	0.403
7	49	0.298	0.265

[a]Based on data from Sherebrin *et al.* (24).
[b]Values determined from our data.
[c]Values corrected to 69 years of age.

CONCLUSIONS

Unlike previous models for the biomechanical behavior of AAA, ours employs a single mathematical description for the entire elastic response. This model conforms to the fibrous structure of the tissue and allows for physical interpretation of the mathematical parameters. Besides modeling the elastic response of arteries, this model may also be useful in characterizing the biomechanical behavior of other soft tissues, since many features of the constitutive structure and response are similar. Data from this investigation suggest that the collagen recruitment rate (or tortuosity) and the failure strengths are altered in the human aorta because of aneurysm and that the mechanical properties are essentially similar between the circumferential and longitudinal directions of an AAA. These results indicate that consideration of the microstructural alterations and peak wall stress should be made in the assessment of AAA severity. Although the present study has provided some new and interesting information on the biomechanical behavior of AAA, more age-matched data for the normal group, as well as the inclusion of circumferentially oriented specimens for this group, would further corroborate the findings. Additionally, to completely validate the present assumptions made regarding the role of elastin and collagen in the biomechanical response of AAA, a similar investigation should be coupled with morphological studies. Morphological parameters such as fiber size, content, orientation, and tortuosity could be examined within each phase of the elastic response described in Fig. 1.

REFERENCES

1. Armentano, R. L., J. Levenson, J. G. Barra, E. I. C. Fischer, G. J. Breitbart, R. H. Pichel, and A. Simon. Assess-

ment of elastin and collagen contribution to aortic elasticity in conscious dogs. *Am. J. Physiol.* 260:H1870–H1877, 1991.

2. Baxter, B. T., V. A. Davis, D. J. Minion, Y. P. Wang, T. G. Lynch, and B. M. McManus. Abdominal aortic aneurysms are associated with altered matrix proteins of the nonaneurysmal aortic segments. *J. Vasc. Surg.* 19:797–802, 1994.
3. Carew, T. E., R. N. Vaishnav, and D. J. Patel. Compressibility of the arterial wall. *Circ. Res.* 23:61–68, 1968.
4. Clark, J. M., and S. Glagov. Transmural organization of the arterial media: The lamellar unit revisited. *Atherosclerosis* 5:19–34, 1985.
5. Cole, C. W. Highlights of an international workshop on abdominal aortic aneurysms. *Can. Med. Assoc. J.* 141:393–395, 1989.
6. Cox, R. H. Passive mechanics and connective tissue composition of canine arteries. *Am. J. Physiol.* 234:H533–H541, 1978.
7. Cronenwett, J. L., S. K. Sargent, H. Wall, M. L. Hawkes, D. H. Freeman, B. J. Dain, J. K. Cure, D. B. Walsh, R. M. Zwolak, M. D. McDaniel, and J. R. Schneider. Variables that affect the expansion rate and outcome of small abdominal aortic aneurysms. *J. Vasc. Surg.* 11:260–268, 1990.
8. Darling, R. C., R. Carlene, R. N. Messina, D. C. Brewster, and L. W. Ottinger. Autopsy study of unoperated abdominal aortic aneurysms: The case for early resection. *Circulation* 56:161–164, 1977.
9. Dobrin, P. B., and R. Mrkvicka. Failure of elastin and collagen as possible critical connective tissue alterations underlying aneurysmal dilation. *Cardiovasc. Surg.* 2:484–488, 1994.
10. Dobrin, P. B. Pathophysiology and pathogenesis of aortic aneurysms. *Surg. Clin. N. Am.* 69:687–703, 1989.
11. Drangova, M., D. W. Holdsworth, C. J. Boyd, P. J. Dunmore, M. R. Roach, and A. Fenster. Elasticity and geometry measurements of vascular specimens using a high resolution laboratory CT scanner. *Physiol. Meas.* 14:277–290, 1993.
12. He, C. M., and M. R. Roach. The composition and mechanical properties of abdominal aortic aneurysms. *J. Vasc. Surg.* 20:6–13, 1994.
13. Lanne, T., B. Sonesson, H. Bengtsson, and D. Gustafsson. Diameter and compliance in the male human abdominal aorta: Influence of age and aortic aneurysm. *Eur. J. Vasc. Surg.* 6:178–184, 1992.
14. Lehninger, A. L. *Biochemistry*. New York: Worth Publishers, 1975, 833 pp.
15. Limet, R., N. Sakalihasan, and A. Albert. Determination of the expansion rate and incidence of rupture of abdominal aortic aneurysm. *J. Vasc. Surg.* 14:540–548, 1991.
16. Macsweeny, S. T., G. Young, R. M. Greenhalgh, and J. T. Powell. Mechanical properties of the aneurysmal aorta. *Br. J. Surg.* 79:1281–1284, 1992.
17. McGee, G. S., B. T. Baxter, V. P. Shively, R. Chisholm, W. J. McCarthy, W. R. Flinn, J. S. Yao, and W. H. Pearce. Aneurysm or occlusive disease factors determining the clinical course of atherosclerosis of the infrarenal aorta. *Surgery* 110:370–375, 1991.
18. Menashi, S., J. S. Campa, R. M. Greenhalgh, and J. T. Powell. Collagen in abdominal aortic aneurysm: Typing, content, and degradation. *J. Vasc. Surg.* 6:578–582, 1987.
19. Ouriel, K., R. M. Green, C. Donayree, C. K. Shortell, J. Elliot, and J. A. DeWeese. An evaluation of new methods of expressing aortic aneurysm size: Relationship to rupture. *J. Vasc. Surg.* 15:12–20, 1992.
20. Park, J. B., and A. S. Hoffman. Interaction of collagen and smooth muscle cells in aortic biomechanics. *Ann. Biomed. Eng.* 6:176–171, 1978.
21. Rizzo, R. J., W. J. McCarthy, S. N. Dixit, M. P. Lilly, V. P. Shively, W. R. Flinn, and J. S. Yao. Collagen types and matrix protein content in human abdominal aortic aneurysms. *J. Vasc. Surg.* 10:365–373, 1989.
22. Roach, M. R., and A. C. Burton. The reason for the shape of the distensibility curves of arteries. *Can. J. Biochem. Physiol.* 35:681–690, 1957.
23. Samila, Z. J., and S. A. Carter. The effect of age on the unfolding of elastin lamellae and collagen fibers with stretch in human carotid arteries. *Can. J. Physiol. Pharmacol.* 59: 1050–1057, 1981.
24. Sherebrin, M. H., J. E. Hegney, and M. R. Roach. Effect of age on the anisotropy of the descending human thoracic aorta determined by uniaxial tensile testing and digestion by NaOH under load. *Can. J. Physiol. Pharmacol.* 67:871–878, 1989.
25. Sterpetti, A. V., R. D. Schultz, R. J. Feldhaus, S. E. Cheng, and D. J. Peetz. Factors influencing enlargement rate of small abdominal aortic aneurysms. *J. Surg. Res.* 43:211–219, 1987.
26. Sumner, D. S., D. E. Hokanson, and D. E. Strandness. Stress-strain characteristics and collagen-elastin content of abdominal aortic aneurysms. *Surg. Gynecol. Obstet.* 130: 459–466, 1970.
17. Vaishnav, R. N., J. T. Young, J. S. Janicki, and D. J. Patel. Nonlinear anisotropic elastic properties of the canine aorta. *Biophys. J.* 12:1008–1027, 1972.
28. Vawter, D. L. Poisson's ratio and incompressibility. *J. Biomech. Eng.* 105:194–195, 1983.
29. Vito, R. P., and J. Hickey. The mechanical properties of soft tissues-II: The elastic response of arterial segments. *J. Biomech.* 13:951–957, 1980.
30. Vorp, D. A., K. R. Rajagopal, P. J. Smolinski, and H. S. Borovetz. Identification of elastic properties of homogeneous orthotropic vascular segments in distention. *J. Biomech.* 28:501–512, 1995.
31. Wolf, Y. G., W. S. Thomas, F. J. Brennan, W. G. Goff, and E. F. Bernstein. Computer topography scanning findings associated with rapid expansion of abdominal aortic aneurysms. *J. Vasc. Surg.* 20:529–535, 1994.

NOMENCLATURE

A = model (Eq. 3) parameter
B = model (Eq. 3) parameter
E_C = contribution to total tissue stiffness by collagen fibers
E_E = contribution to total tissue stiffness by elastin fibers

K = model (Eq. 3) parameter
a = current (deformed) cross-sectional area of the specimen
a_0 = initial (undeformed) cross-sectional area of the specimen
f = applied force
Δl = change in length of the specimen
l_0 = original length of specimen at zero extension
v = current volume of the specimen
v_0 = initial volume of the specimen
α = model (Eq. 18) parameter
β = model (Eq. 18) parameter
ϵ = strain
σ = Cauchy stress
σ_u = ultimate strength
σ_y = yield strength